EXACT BOUNDARY CONDITION PERTURBATION FOR EIGENSOLUTIONS OF THE WAVE EQUATION

R. G. PARKER

Department of Mechanical Engineering, Ohio State University, 206 West 18th Avenue, Columbus, OH 43210-1107, U.S.A.

AND

C. D. MOTE, JR.

Department of Mechanical Engineering, University of California, Berkeley, 2440 Bancroft Way, Berkeley, CA 94720-4200, U.S.A.

A perturbation method is presented to analytically calculate eigensolutions of the two-dimensional wave equation when asymmetric perturbations are present in the boundary conditions. The unique feature of the method is that the sequence of boundary value problems governing the eigensolution perturbations are solved exactly through fifth order perturbation. Two classes of asymmetry are considered: irregular domain shapes that cannot be treated by analytical means, and variation of the boundary conditions along the boundary. The unperturbed eigensolutions are those for an annular domain with axisymmetric boundary conditions. Irregularly shaped domains are studied in detail to demonstrate the method and the accuracy of the results, which are compared with exact values for the elliptical and rectangular domain cases. The results show excellent agreement with these known solutions for large shape distortions, an achievement resulting from the extension to higher order perturbation. Fourier representation of the boundary asymmetries allows analysis of arbitrary distributions of asymmetry. Additionally, the exact perturbation solution retains the explicit parameter dependence of continuous system analysis, generates simple expressions for the perturbed eigensolutions, addresses all distinct and degenerate axisymmetric system eigensolutions, and requires minimal computation and programming.

© 1998 Academic Press Limited

1. INTRODUCTION

The wave equation

$$-\mathbf{V}^2 q + q_{tt} = f(x, y, t), \quad \overline{P}; \qquad q + \beta q_n = 0, \quad \partial\overline{P}; \tag{1}$$

is arguably the most widely-studied differential equation in science and engineering. It is used to model physical systems in diverse fields such as acoustics, wave propagation, vibration, electromagnetics, fluid mechanics, heat transfer, and diffusion. Eigensolutions of the two-dimensional wave equation, governed by the Helmholtz equation, are the focus of this paper. A perturbation method is presented to analytically calculate eigensolutions when asymmetric perturbations are present in the boundary conditions. The axisymmetric, annular domain case serves as the unperturbed problem. Possible boundary condition perturbations include deviation of the domain $\overline{P}$ from annular and variation of the parameter β along the boundary $\partial\overline{P}$. The eigensolution perturbations are determined *exactly*, and their algebraic simplicity allows extension of the perturbation through fifth

order. Both distinct and degenerate eigenvalues of the unperturbed problem are examined. Boundary condition asymmetry splits the degenerate unperturbed eigenvalues. Simple rules are derived predicting this splitting at both first and second orders of perturbation. To illustrate the method and quantify its accuracy, the case of domain shape perturbation from circular is addressed in detail and comparisons are made with the exact solutions for elliptical and rectangular domains.

Methods used to analyze eigensolutions of the wave equation on irregular domains have been primarily numerical; for example finite element, finite difference and others. In addition to an extensive summary of theoretical results, Kuttler and Sigillito [1] provide a comprehensive review (142 references) of the application of these and other less popular methods. Mazumdar also reviews approximate methods invoked for this problem [2–4]. The above methods can be augmented by conformally mapping the irregular domain to a circle [5]. In the spirit of perturbation, Joseph [6] employed a parameter differentiation method to obtain derivatives of the distinct eigenvalues as the domain changes. The requirement of a smooth mapping function from the unperturbed domain to the irregular one and the restriction to distinct eigenvalues of the unperturbed problem limit its applicability. By assuming expressions for the lines of constant deflection in the fundamental eigenfunction, Mazumdar obtained estimates for the fundamental eigenvalue for arbitrarily shaped domains [7]. Accuracy of this method depends on the availability of a good estimate of the lines of constant deflection. Morse and Feshbach [8] used a perturbation analysis different from that presented herein to study the Helmholtz equation on irregular domains. Expansion of the eigenfunction perturbations in infinite series of the unperturbed eigenfunctions leads to a convergence problem restricting the analysis to second order perturbation in the eigenvalue and first order in the eigenfunction. Nayfeh used a perturbation formulation similar to that of this work to calculate the eigenvalue perturbation to first order; no eigenfunction perturbations are presented [9]. This work draws on the results of Parker and Mote [10, 11], where a formal procedure for obtaining exact eigensolution perturbations is developed.

2. EIGENSOLUTION PERTURBATION FORMULATION

The eigenvalue problem resulting from separation of the spatial and temporal dependence in equation (1) by the assumption $q = p(R, \theta)\, \mathrm{e}^{i\Omega t}$ is

$$-\mathbf{V}^2 p - \Omega^2 p = 0, \quad \bar{P}; \qquad p + \beta p_n = 0, \qquad \partial \bar{P}: \partial \bar{P}_i \cup \partial \bar{P}_o ; \qquad \text{(2a, b)}$$

where subscript n denotes the normal derivative. Two classes of asymmetry are examined that normally preclude exact determination of the exact solution to (2): irregular $\bar{P}$ and variation of β along $\partial \bar{P}$. These asymmetries are treated as perturbations of the axisymmetric, annular domain eigenvalue problem.

2.1. IRREGULAR DOMAIN SHAPE

The two-dimensional, doubly-connected domain $\bar{P}$ in Figure 1 is $\bar{P} : R_i(\theta) < R < R_o(\theta), 0 \leqslant \theta < 2\pi$. The deviations of the boundaries $\partial \bar{P}_i$ and $\partial \bar{P}_o$ from circular are

$$\varepsilon \bar{g}_i(\theta) \equiv R_i(\theta) - \bar{R}_i, \qquad \varepsilon \bar{g}_o(\theta) \equiv R_o(\theta) - \bar{R}_o, \qquad \text{(3)}$$

where $\bar{R}_i$ and $\bar{R}_o$ are the average radii of the inner and outer boundaries. The variables q, p, and t in equations (1) and (2) are dimensionless; scaling the domain with the additional dimensionless variables
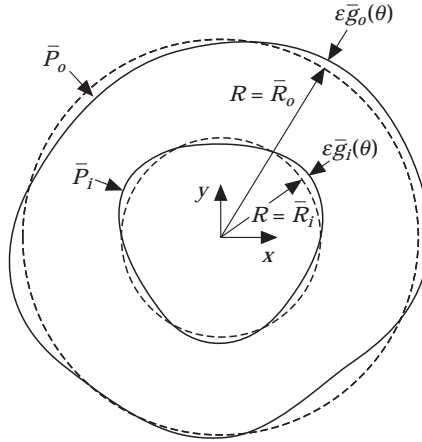
Figure 1. The irregular domain is denoted by the solid lines, and the annular domain for perturbation by the dashed lines. The radii of the dashed circles equal the average radii of the irregular bounding curves.

$$r = \frac{R}{\bar{R}_o}; \qquad \gamma = \frac{\bar{R}_i}{\bar{R}_o}, \qquad \bar{\omega} = \bar{R}_o\,\Omega, \qquad \varepsilon g_o\,(\theta) = \frac{\varepsilon \bar{g}_o\,(\theta)}{\bar{R}_o}, \qquad \varepsilon g_i\,(\theta) = \frac{\varepsilon \bar{g}_i\,(\theta)}{\bar{R}_o} \qquad (4)$$

yields the eigenvalue problem for constant $\beta = \beta_o$

$$-\mathbf{V}^2 p - \bar{\omega}^2 p = 0, \quad \hat{P}; \qquad p + \beta_o\, p_n = 0, \quad \partial \hat{P}; \qquad\qquad (5a, b)$$

where $\hat{P} : \gamma + \varepsilon g_i\,(\theta) < r < 1 + \varepsilon g_o\,(\theta),\ 0 \leqslant \theta < 2\pi$.

Boundary quantities on $\partial \hat{P}$ are approximated by Taylor series expansion about $r = \gamma,\ 1$. For example,

$$p\,|_{r=1+\varepsilon g_o} = p\,|_{r=1} + (\varepsilon g_o)p_r\,|_{r=1} + 1/2!(\varepsilon g_o)^2 p_{rr}\,|_{r=1} + 1/3!(\varepsilon g_o)^3 p_{rrr}\,|_{r=1} + \cdots. \qquad (6)$$

A similar expansion is developed for $p\,|_{\partial \hat{P}_i}$. The expansions $p_n\,|_{\partial \hat{P}_{i,o}}$ require asymptotic expansion of p_n in terms of derivatives with respect to the polar co-ordinates r and θ [12]. Introduction of the expansions for p and p_n on $\partial \hat{P}$ into equation (5b) yields

$$-\mathbf{V}^2 p - \bar{\omega}^2 p = 0, \qquad P : \gamma \leqslant r < 1,\ 0 \leqslant \theta < 2\pi, \qquad\qquad (7a)$$

$$(p - \beta_o\, p_r) + \varepsilon \bar{C} p + \varepsilon^2 \bar{D} p + \varepsilon^3 \bar{E} p + \cdots = 0, \qquad r = \gamma, \qquad\qquad (7b)$$

$$(p + \beta_o\, p_r) + \varepsilon \hat{C} p + \varepsilon^2 \hat{D} p + \varepsilon^3 \hat{E} p + \cdots = 0, \qquad r = 1, \qquad\qquad (7c)$$

where $\bar{C}, \bar{D}, \hat{C}, \hat{D}, \ldots$ are linear boundary operators with variable coefficients depending on $g_i\,(\theta)$ and $g_o\,(\theta)$.

2.2. VARIABLE β ALONG ∂P

For annular domains with $\beta \to \beta_o + \varepsilon \beta(\theta)$, the eigenvalue problem becomes

$$-\mathbf{V}^2 p - \bar{\omega}^2 p = 0, \qquad P : \gamma \leqslant r < 1,\ 0 \leqslant \theta < 2\pi, \qquad\qquad (8a)$$

$$(p - \beta_o\, p_r) - \varepsilon \beta(\theta) p_r = (p - \beta_o\, p_r) + \varepsilon \bar{C} p = 0, \qquad r = \gamma, \qquad\qquad (8b)$$

$$(p + \beta_o\, p_r) + \varepsilon \beta(\theta) p_r = (p + \beta_o\, p_r) + \varepsilon \hat{C} p = 0, \qquad r = 1, \qquad\qquad (8c)$$

which is of form identical to equation (7).

Eigensolutions of equation (7) are sought where the boundary perturbations may result from either or both of the asymmetries discussed above. The eigensolutions are represented as asymptotic series in the small parameter ε:

$$\bar{\omega}^2 = \omega^2 + \varepsilon\mu + \varepsilon^2\eta + \varepsilon^3\kappa + \varepsilon^4\chi + \varepsilon^5\sigma + O(\varepsilon^6), \tag{9}$$

$$p = u + \varepsilon v + \varepsilon^2 w + \varepsilon^3 s + \varepsilon^4 t + \varepsilon^5 z + O(\varepsilon^6). \tag{10}$$

Subsequent analysis shows that confinement of the perturbation terms to the boundary conditions ensures that the Bessel and trigonometric forms of the eigenfunction perturbations in equation (10) do not depend on the boundary perturbations. Only the coefficients of these Bessel and trigonometric functions depend on the boundary condition operators. Because of this essential point, the method presented in the sequel for finding exact solutions for the eigensolution perturbations on irregular domains can be readily applied to find exact eigensolution perturbations for any problem of the form (7).

With the inner product $\langle e, f \rangle = \iint_P ef \, dA$, the normalization $\langle p, p \rangle = 1$ and equation (10) give

$$\langle u, v \rangle = 0, \quad \langle u, w \rangle = -\tfrac{1}{2}\langle v, v \rangle, \quad \langle u, s \rangle = -\langle v, w \rangle, \quad \langle u, t \rangle = -\langle v, s \rangle - \tfrac{1}{2}\langle w, w \rangle, \tag{11}$$

The eigenvalue perturbations μ, η, κ, χ, and σ are determined subsequently in terms of the boundary conjunct $J(e, f)$:

$$J(e, f) = \langle -\nabla^2 e, f \rangle - \langle e, -\nabla^2 f \rangle = \int_{\partial P} [ef_n - fe_n] \, d\hat{s}. \tag{12}$$

3. IRREGULAR DOMAIN EIGENSOLUTION PERTURBATION

The solution procedure for eigenvalue problems of the form (7) is demonstrated by examining an irregularly shaped domain with outer boundary $\partial\bar{P}$ and boundary condition $p|_{\partial\bar{P}} = 0$. Use of equations (4) and (6) yields

$$-\nabla^2 p - \bar{\omega}^2 p = 0, \qquad P: 0 \leqslant r < 1, \quad 0 \leqslant \theta < 2\pi, \tag{13a}$$

$$p + \varepsilon g p_r + 1/2!(\varepsilon g)^2 p_{rr} + 1/3!(\varepsilon g)^3 p_{rrr} + 1/4!(\varepsilon g)^4 p_{rrrr} + 1/5!(\varepsilon g)^5 p_{rrrrr} = 0, \quad r = 1, \tag{13b}$$

where the subscript o denoting the outer boundary has been omitted. Substitution of equations (9, 10) into equation (13) yields the sequence of perturbation problems

$$-\nabla^2 u - \omega^2 u = 0, \quad P; \qquad u = 0, \qquad \partial P, \tag{14a, b}$$

$$-\nabla^2 v - \omega^2 v = \mu u, \quad P; \qquad v = -g u_r, \quad \partial P; \tag{15a, b}$$

$$-\nabla^2 w - \omega^2 w = \mu v + \eta u, \quad P; \qquad w = -g v_r - (\tfrac{1}{2})g^2 u_{rr}, \quad \partial P; \tag{16a, b}$$

$$-\nabla^2 s - \omega^2 s = \mu w + \eta v + \kappa u, \quad P; \qquad s = -g w_r - (\tfrac{1}{2})g^2 v_{rr} - (\tfrac{1}{6})g^3 u_{rrr}, \quad \partial P; \tag{17a, b}$$

$$-\nabla^2 t - \omega^2 t = \mu s + \eta w + \kappa v + \chi u, \quad P; \tag{18a}$$

$$t = -g s_r - (\tfrac{1}{2})g^2 w_{rr} - (\tfrac{1}{6})g^3 v_{rrr} - (\tfrac{1}{24})g^4 u_{rrrr}, \quad \partial P; \tag{18b}$$

$$-\nabla^2 z - \omega^2 z = \mu t + \eta s + \kappa w + \chi v + \sigma u, \quad P; \tag{19a}$$

$$z = -g t_r - (\tfrac{1}{2})g^2 s_{rr} - (1/6)g^3 w_{rrr} - (\tfrac{1}{24})g^4 v_{rrrr} - (\tfrac{1}{120})g^5 u_{rrrrr}, \quad \partial P. \tag{19b}$$

Solution of equation (14) gives the orthonormal unperturbed eigenfunctions

$$u_{m0} = (1/\pi^{1/2}) \, J_0(\omega_{m0} r)/J_1(\omega_{m0}) = R_{m0}(r), \qquad m \geqslant 0; \tag{20}$$

$$u_{mn}^{c,s} = \left(\frac{2}{\pi}\right)^{1/2} \frac{\mathrm{J}_n\,(\omega_{mn}\,r)}{\mathrm{J}_{n+1}\,(\omega_{mn})} \begin{Bmatrix} \cos\ n\theta \\ \sin\ n\theta \end{Bmatrix} = R_{mn}\,(r) \begin{Bmatrix} \cos\ n\theta \\ \sin\ n\theta \end{Bmatrix}, \quad m \geqslant 0,\ n > 0; \tag{21}$$

where m and n denote the number of nodal circles and nodal diameters in the eigenfunction. The unperturbed eigenvalue ω_{mn} is the $(m+1)$th root of the characteristic equation $\mathrm{J}_n\,(\omega) = 0$. ω_{mn} is a distinct eigenvalue for $n = 0$ and a degenerate eigenvalue of multiplicity two for $n \geqslant 1$. u_{mn}^{cs} are orthonormal eigenfunctions associated with the degenerate eigenvalues.

For the circular domain P, the boundary conjunct (12) is

$$J(e,f) = \int_0^{2\pi} [ef_r - fe_r]_{r=1}\ \mathrm{d}\theta. \tag{22}$$

The following relations are used subsequently:

$$R'_{m0}\,(1) = -\frac{\omega_{m0}}{\pi^{1/2}}, \qquad R''_{m0}\,(1) = \frac{\omega_{m0}}{\pi^{1/2}}, \qquad R'_{mn}\,(1) = -\left(\frac{2}{\pi}\right)^{1/2}\omega_{mn},$$

$$R''_{mn}\,(1) = \left(\frac{2}{\pi}\right)^{1/2}\omega_{mn}, \tag{23}$$

$$g(\theta) = \sum_{j=1}^{\infty} g_j^c\,\cos j\theta + \sum_{j=1}^{\infty} g_j^s\,\sin j\theta, \tag{24}$$

$$G(\theta) = g^2(\theta) = G_0 + \sum_{j=1}^{\infty} G_j^c\,\cos j\theta + \sum_{j=1}^{\infty} G_j^s\,\sin j\theta. \tag{25}$$

Use of the Fourier representation (24) allows treatment of *arbitrary* boundary shapes, including kinked or discontinuous boundaries. The constant term in equation (24) vanishes because $\bar{R}$ is the average radius of the boundary.

4. SOLUTION OF PERTURBATION EQUATIONS

4.1. DISTINCT EIGENVALUE PERTURBATION

Consider perturbation of a distinct unperturbed eigensolution $(\omega_{m0},\,u_{m0})$ (the subscript $m0$ will be omitted in the sequel). Using solvability conditions for the perturbation problems (15–19), Parker and Mote have presented formal expressions for the distinct eigenvalue perturbations in terms of the boundary conjunct [10, 11]:

$$\mu = -J(u, v), \qquad \eta = -J(u, w), \qquad \kappa = -\mu\langle u, w\rangle - J(u, s),$$

$$\chi = -\mu\langle u, s\rangle - \eta\langle u, w\rangle - J(u, t), \qquad \sigma = -\mu\langle u, t\rangle - \eta\langle u, s\rangle - \kappa\langle u, w\rangle - J(u, z) \tag{26}$$

4.1.1. First order perturbation

The first order eigenvalue perturbation μ is evaluated from equations (26a), (22), (14b), (15b), (20), and (24):

$$\mu = \int_0^{2\pi} [u_r\,v]_{r=1}\ \mathrm{d}\theta = -[R'_0\,(1)]^2 \int_0^{2\pi} g\ \mathrm{d}\theta = 0. \tag{27}$$

The result $\mu = 0$ substantially simplifies subsequent calculations. It results because the radius of the unperturbed circular domain is the mean radius of the irregular domain.

In their treatment of boundary shape perturbation of the Helmholtz equation, Morse and Feshbach [8] noted convergence difficulties when the eigenfunction perturbation is expanded in a series of the unperturbed eigenfunctions. For the similar case of plate boundary shape perturbation, Parker and Mote [12] encountered a divergent series for the second order eigenvalue perturbation when the first order eigenfunction perturbation is expanded in a series of the unperturbed eigenfunctions. These problems do not occur when the exact solution for the eigenfunction perturbation is determined. Furthermore, the exact solution is more accurate, computationally efficient, and notationally convenient than the infinite series expansion. In the sequel, exact eigenfunction perturbation solutions are determined through fourth order perturbation, thereby allowing exact calculation of the fifth order eigenvalue perturbation.

The eigenfunction perturbation $v(r, \theta)$ is decomposed as

$$v = cu + v^h + v^p. \tag{28}$$

The first term results because u is a non-trivial solution of the homogeneous form of equation (15a, b); c is a constant to be determined. The second term is the general solution of the homogeneous form of equation (15a). The third term of equation (28) is a particular solution of the inhomogeneous equation (15a). Because of equation (27),

$$v^p = 0. \tag{29}$$

Additionally,

$$v^h = \sum_{j=1}^{\infty} \mathrm{J}_j\,(\omega r)\,[B_j \cos j\theta + C_j \sin j\theta], \tag{30}$$

where the $j = 0$ term is omitted because its contribution is included in the first term of equation (28). The coefficients in equation (30) are calculated from equation (15b):

$$B_j = \omega g_j^c \,/\pi^{1/2}\mathrm{J}_j\,(\omega), \qquad C_j = \omega g_j^s\,/\pi^{1/2}\mathrm{J}_j\,(\omega), \tag{31}$$

where g_j^c and g_j^s are from equations (24). Substitution of equation (28) into the normalization condition (11a) yields

$$c = -\langle u, v^h + v^p \rangle = 0 \tag{32}$$

and the solution for v is complete.

4.1.2. Second order perturbation

The second order eigenvalue perturbation η is evaluated from equations (26b), (22), (14b), (16b), (20), (28–32), (24), and (25):

$$\eta = \int_0^{2\pi} [u_r\,(-gv_r - \tfrac{1}{2}\,g^2 u_{rr})]_{r=1}\,\mathrm{d}\theta = \omega^2 \left\{ G_0 + \sum_{j=1}^{\infty} \left[j - \omega \frac{J_{j+1}\,(\omega)}{J_j\,(\omega)} \right](g_j^c)^2 + (g_j^s)^2 \right] \right\} \tag{33}$$

The solution of equation (16) is decomposed as

$$w = du + w^h + w^p \tag{34}$$

where the definitions of the terms in equation (34) are analogous to those in equation (28), and

$$w^p = -(\eta r/(4\pi)^{1/2}\omega)\, J_1(\omega r)/J_1(\omega), \qquad w^h = \sum_{j=1}^{\infty} J_j(\omega r)\, [E_j \cos j\theta + F_j \sin j\theta]. \quad (35, 36)$$

The coefficients E_j and F_j in equation (36) are determined from equation (16b):

$$E_j = -\frac{\omega}{(4\pi)^{1/2} J_j(\omega)} \left[G_j^c + \sum_{m=1}^{\infty} \left[m - \omega \frac{J_{m+1}(\omega)}{J_m(\omega)} \right] \right.$$

$$\times \left. \begin{cases} g_m^c\,(g_{m+j}^c + g_{m-j}^c) + g_m^s\,(g_{m+j}^s + g_{m-j}^s) & m > j \\ g_m^c\,(g_{m+j}^c + g_{j-m}^c) + g_m^s\,(g_{m+j}^s - g_{j-m}^s) & m < j \\ g_m^c\, g_{2m}^c + g_m^s\, g_{2m}^s & m = j \end{cases} \right],$$

$$F_j = -\frac{\omega}{(4\pi)^{1/2} J_j(\omega)} \left[G_j^s + \sum_{m=1}^{\infty} \left[m - \omega \frac{J_{m+1}(\omega)}{J_m(\omega)} \right] \right.$$

$$\times \left. \begin{cases} g_m^c\,(g_{m+j}^s - g_{m-j}^s) - g_m^s\,(g_{m+j}^c - g_{m-j}^c) & m > j \\ g_m^c\,(g_{m+j}^s + g_{j-m}^s) - g_m^s\,(g_{m+j}^c - g_{j-m}^c) & m < j \\ g_m^c\, g_{2m}^s - g_m^s\, g_{2m}^c & m = j \end{cases} \right].$$

From the normalization (11b),

$$d = -\tfrac{1}{2}\langle v, v \rangle - \langle u, w^p \rangle$$

$$= -\frac{\omega^2}{2} \sum_{m=1}^{\infty} \left[1 - \frac{2m}{\omega} \frac{J_{m+1}(\omega)}{J_m(\omega)} + \frac{J_{m+1}^2(\omega)}{J_m^2(\omega)} \right] [(g_m^c)^2 + (g_m^s)^2] - \frac{\eta}{2\omega^2}. \qquad (37)$$

The particular solution (35) is the critical component of the solution (34). With w^p known, calculation of E_j and F_j is straightforward for any perturbed boundary conditions (7b, c).

Equations (27–37) provide exact, closed-form expressions for both the eigenvalue and eigenfunction perturbations through second order. Their simplicity is remarkable given that they apply for an *arbitrary* deviation in boundary shape.

4.1.3. *Third order perturbation*

The third order eigenvalue perturbation (26c) is

$$\kappa = -J(u, s) = \int_0^{2\pi} [u_r\,(-g w_r - \tfrac{1}{2} g^2 v_{rr} - (\tfrac{1}{6}) g^3 u_{rrr})]_{r=1}\, d\theta. \qquad (38)$$

Derivation of a closed form expression for κ is analogous to equation (33) and straightforward. The value of the expression is minimal, however, because equation (38) can be evaluated easily using computer algebra software for a specified $g(\theta)$. Little insight can be gained from the algebraic details at third order perturbation.

The third order eigenfunction perturbation $s(r, \theta)$ is

$$s = eu + s^h + s^p. \tag{39}$$

A particular solution for the κu term in equation (17a) is known by analogy with equation (35):

$$s_1^p = -(\kappa r/(4\pi)^{1/2}\omega) (J_1(\omega r)/J_1(\omega)). \tag{40}$$

A particular solution associated with the ηv term of equation (17a) is

$$s_2^p = -\frac{nr}{2\omega} \sum_{j=1}^{\infty} J_{j+1}(\omega r) [B_j \cos j\theta + C_j \sin j\theta]. \tag{41}$$

Finally,

$$s^p = s_1^p + s_2^p. \tag{42}$$

As in equations (30) and (36),

$$s^h = \sum_{j=1}^{\infty} J_j(\omega r) [H_j \cos j\theta + L_j \sin j\theta], \tag{43}$$

where numerical evaluation of H_j and L_j for specified $g(\theta)$ is readily achieved. e in equation (39) is found from (11c)

$$e = -\langle v, w \rangle - \langle u, s^p \rangle. \tag{44}$$

4.1.4. Fourth order perturbation

The fourth order eigenvalue perturbation χ is found from equation (26d):

$$\chi = -\eta d + \eta^2/2\omega^2 - J(u, t). \tag{45}$$

The fourth order eigenfunction perturbation $t(r, \theta)$ is

$$t = fu + t^h + t^p. \tag{46}$$

Expansion of equation (18a) yields

$$-\mathbf{V}^2 t - \omega^2 t = (\chi + \eta d)u + \kappa v^h + \eta w^h + \eta w^p, \quad P. \tag{47}$$

A particular solution of equation (47) is

$$t^p = t_1^p + r_2^p + t_3^p + t_4^p, \qquad t_1^p = -\frac{(\chi + \eta d)r}{(4\pi)^{1/2}\omega} \frac{J_1(\omega r)}{J_1(\omega)}, \tag{48, 49}$$

$$t_2^p = -\frac{\kappa r}{2\omega} \sum_{j=1}^{\infty} J_{j+1}(\omega r) [B_j \cos j\theta + C_j \sin j\theta], \tag{50}$$

$$t_3^p = -\frac{\eta r}{2\omega} \sum_{j=1}^{\infty} J_{j+1}(\omega r) [E_j \cos j\theta + F_j \sin j\theta], \tag{51}$$

$$t_4^p = -\frac{\eta^2 r}{(64\pi)^{1/2}\omega^3 J_1(\omega)} [\omega r J_0(\omega r) - 2J_1(\omega)], \tag{52}$$

where t_4^p is the only "new" particular solution not determined by analogy with previous particular solutions. Coefficients of t^h are calculated from equation (18b). The normalization (11d) gives

$$f = -\tfrac{1}{2}\langle w, w \rangle - \langle v, s \rangle - \langle u, t^p \rangle. \tag{53}$$

4.1.5. *Fifth order perturbation*

From equation (26e), the fifth order eigenvalue perturbation σ is

$$\sigma = -\eta e - \kappa d + n\kappa/\omega^2 - J(u, z). \tag{54}$$

4.2. DEGENERATE EIGENVALUE PERTURBATION

Consider perturbation of a degenerate unperturbed eigenvalue ω_{mn} and the associated n nodal diameter orthonormal eigenfunctions $u_{mn}^{c,s}$ (21) (the subscript mn will henceforth be omitted). Because of the eigenvalue degeneracy, the unperturbed eigenfunction u is an element in the linear space spanned by u^c and u^s:

$$u = a_c u^c + a_s u^s; \tag{55}$$

where a_c and a_s are determined subsequently. The normalization $\langle u, u \rangle = 1$ requires

$$a_c^2 + a_s^2 = 1. \tag{56}$$

Boundary condition asymmetry splits the degenerate unperturbed eigenvalue and fixes the coefficients a_c and a_s in equation (55). These effects *might* occur at first order perturbation, though, if not, they are predicted at some higher order perturbation.

Because u^c and u^s are solutions of the homogeneous forms of equations (15–19), two solvability conditions must be satisfied at each order of perturbation. The method of Parker and Mote [10] is followed.

4.2.1. *First order perturbation*

The solvability conditions for equation (15) yield

$$a_c \mu = -J(u^c, v), \qquad a_s \mu = -J(u^s, v). \tag{57}$$

Evaluation of equations (57) yields a symmetric, algebraic eigenvalue problem,

$$-\omega^2 \begin{bmatrix} g_{2n}^c & g_{2n}^s \\ g_{2n}^s & -g_{2n}^c \end{bmatrix} \begin{Bmatrix} a_c \\ a_s \end{Bmatrix} = \mu \begin{Bmatrix} a_c \\ a_s \end{Bmatrix} \rightarrow \mathbf{Da} = \mu \mathbf{a},$$

$$\mu_{1,2} = \pm \omega^2 [(g_{2n}^c)^2 + (g_{2n}^s)^2]^{1/2}. \tag{58}$$

The eigenvalues of $\mathbf{D}$ are the first order perturbations of ω. The eigenvectors of $\mathbf{D}$ fix the coefficients in equation (55). The degenerate eigenvalue splits into distinct eigenvalues as a result of boundary asymmetry if and only if the μ are distinct. The magnitude of μ for an n nodal diameter eigenvalue is proportional to $[(g_{2n}^c)^2 + (g_{2n}^s)^2]^{1/2}$. This leads to the splitting rule: If either or both of g_{2n}^c and g_{2n}^s are non-zero, the n nodal diameter eigenvalues split at first order perturbation; otherwise the eigenvalues remain degenerate. When no first order splitting occurs, $\mu = 0$ but a_c and a_s remain undetermined.

The eigenfunction perturbation $v(r, \theta)$ is decomposed as

$$v = c_c u^c + c_s u^s + v^h + v^p, \tag{59}$$

where the first two terms result from the two independent solutions of the homogeneous form of equation (15). Particular and homogeneous solutions of equation (15a) are

$$v^p = (\mu r/(2\pi)^{1/2}\omega)\mathrm{J}_{n+1}(\omega r)/\mathrm{J}_{n+1}(\omega)(a_c \cos n\theta + a_s \sin n\theta), \tag{60}$$

$$v^h = \sum_{j=0, j \neq n}^{\infty} \mathrm{J}_j(\omega r)[B_j \cos j\theta + C_j \sin j\theta], \tag{61}$$

where the $j = n$ term of equation (61) is included in the first terms of equation (59). Using equation (15b),

$$B_j = \frac{\omega}{(2\pi)^{1/2}J_j(\omega)} \begin{cases} a_c\,(g^c_{j+n} + g^c_{j-n}) + a_s\,(g^s_{j+n} - g^s_{j-n}), & j > n, \\ a_c\,(g^c_{j+n} + g^c_{n-j}) + a_s\,(g^s_{j+n} + g^s_{n-j}), & j < n, \\ a_c\,g^c_n + a_s\,g^s_n, & j = 0, \end{cases} \tag{62a}$$

$$C_j = \frac{\omega}{(2\pi)^{1/2}J_j(\omega)} \begin{cases} a_c\,(g^s_{j+n} + g^s_{j-n}) - a_s\,(g^c_{j+n} - g^c_{j-n}), & j > n, \\ a_c(g^s_{j+n} - g^s_{n-j}) - a_s\,(g^c_{j+n} - g^c_{n-j}), & j < n. \end{cases} \tag{62b}$$

Coefficients c_c and c_s completing the solution (59) are calculated at second order perturbation, just as a_c and a_s of equation (55) are calculated at first order perturbation.

4.2.2. *Second order perturbation*

The two solvability conditions for (16) and (11a) yield

$$\begin{bmatrix} \mu + \omega^2 g^c_{2n} & \omega^2 g^s_{2n} & \omega^2 a_c \\ \omega^2 g^s_{2n} & \mu - \omega^2 g^c_{2n} & \omega^2 a_s \\ \omega^2 a_c & \omega^2 a_s & 0 \end{bmatrix} \begin{Bmatrix} c_c \\ c_s \\ \eta/\omega^2 \end{Bmatrix} = \begin{Bmatrix} [\mu^2(n+1)/2\omega^2]a_c - \tilde{J}(u^c, w) \\ [\mu^2(n+1)/2\omega^2]a_s - \tilde{J}(u^s, w) \\ [\mu(n+1)/2] \end{Bmatrix}, \tag{63}$$

$$\tilde{J}(u^c, w) = J(u^c, w)|_{c_c = c_s = 0}$$

$$= a_c \left\{ -\frac{\mu n}{2} g^c_{2n} - \omega^2(G_0 + \tfrac{1}{2}G^c_{2n}) - \frac{\omega^2}{2} \sum_{j=0, j \neq n}^{\infty} \left[j - \omega \frac{J_{j+1}(\omega)}{J_j(\omega)} \right]\alpha_j \right\}$$

$$+ a_s \left\{ -\frac{\mu n}{2} g^s_{2n} - \omega^2(\tfrac{1}{2}G^s_{2n}) - \omega^2 \sum_{j=0, j \neq n}^{\infty} \left[j - \omega \frac{J_{j+1}(\omega)}{J_j(\omega)} \right]\beta_j \right\} = a_c\,X + a_s\,Y,$$

$$\tag{64a}$$

$$\tilde{J}(u^s, w) = J(u^s, w)|_{c_c = c_s = 0} = a_c \left\{ -\frac{\mu n}{2} g^s_{2n} - \omega^2(\tfrac{1}{2}G^s_{2n}) - \omega^2 \sum_{j=0, j \neq n}^{\infty} \left[j - \omega \frac{J_{j+1}(\omega)}{J_j(\omega)} \right]\beta_j \right\}$$

$$+ a_s \left\{ -\frac{\mu n}{2} g^c_{2n} - \omega^2(G_0 + \tfrac{1}{2}G^c_{2n}) - \frac{\omega^2}{2} \sum_{j=0, j \neq n}^{\infty} \left[j - \omega \frac{J_{j+1}(\omega)}{J_j(\omega)} \right]\Gamma_j \right\}$$

$$= a_c\,Y + a_s\,Z, \tag{64b}$$

$$\alpha_j = \begin{cases} (g^c_{j+n} + g^c_{j-n})^2 + (g^s_{j+n} + g^s_{j-n})^2 \\ (g^c_{j+n} + g^c_{n-j})^2 + (g^s_{j+n} - g^s_{n-j})^2, \\ 2(g^c_n)^2 \end{cases} \quad \beta_j = \begin{cases} -g^c_{j+n} g^s_{j-n} + g^c_{j-n} g^s_{j+n}, & j > n, \\ g^c_{j+n} g^s_{n-j} + g^c_{n-j} g^s_{j+n}, & j < n, \\ g^c_n g^s_n, & j = 0, \end{cases}$$

$$\Gamma_j = \begin{cases} (g^c_{j+n} - g^c_{j-n})^2 + (g^s_{j+n} - g^s_{j-n})^2 \\ (g^c_{j+n} - g^c_{n-j})^2 + (g^s_{j+n} + g^s_{n-j})^2, \\ 2(g^s_n)^2 \end{cases} \quad \delta_j = \begin{cases} g^c_{j+n} g^c_{j-n} + g^s_{j+n} g^s_{j-n}, & j > n, \\ g^c_{j+n} g^c_{n-j} - g^s_{j+n} g^s_{n-j}, & j < n, \\ \frac{1}{2}[(g^c_n)^2 - (g^s_n)^2], & j = 0 \end{cases}$$

$\delta_j = (\frac{1}{4})(\alpha_j - \Gamma_j)$ is used in equation (66). The operator in equation (63) is invertible if and only if the unperturbed eigenvalue splits at first order perturbation; c_c, c_s, and η are calculable from equation (63). If $g^c_{2n} = g^s_{2n} = 0$, then $\mu = 0$, the operator in equation (63) is singular, and a_c and a_s are unknown. In this case, the component equations of equation (63) yield

$$a_c \tilde{J}(u^s, w) - a_s \tilde{J}(u^c, w) = Y(a_c^2 - a_s^2) + (Z - X)a_c a_s = 0,$$

$$\eta = -a_c \tilde{J}(u^c, w) - a_s \tilde{J}(u^s, w) = -Xa_c^2 - 2Ya_c a_s - Za_s^2, \tag{65}$$

where X, Y, and Z are defined in equation (64). The first of equations (65) and (56) can be solved for two unique $\mathbf{a} = (a_c \ a_s)^{\mathrm{T}}$ if and only if one or both of the following inequalities hold:

$$Y \neq 0 \rightarrow \frac{1}{2} G^s_{2n} + \sum_{j=0, j \neq n}^{\infty} \left[j - \omega \frac{J_{j+1}(\omega)}{J_j(\omega)} \right] \beta_j \neq 0,$$

$$X \neq Z \rightarrow \frac{1}{2} G^s_{2n} + \sum_{j=0, j \neq n}^{\infty} \left[j - \omega \frac{J_{j+1}(\omega)}{J_j(\omega)} \right] \delta_j \neq 0; \tag{66}$$

η is then calculated from equation (65b). Equations (66) are second order eigenvalue splitting rules: if either or both of equations (66) are satisfied, the n nodal diameter eigenvalues split at second order; otherwise they do not. When $Y = 0$ and $X = Z$, equations (65b) and (56) yield $\eta = -X = -Z$ while equation (65a) is identically satisfied. Thus, η is calculable despite the lack of second order splitting and the continuing indeterminacy of $a_{c,s}$. In the sequel, one assumes the degenerate eigenvalues split at first order. If they do not, the development described by Parker and Mote [11] is required.

The second order eigenfunction perturbation $w(r, \theta)$ is

$$w = d_c u^c + d_s u^s + w^h + w^p, \tag{67}$$

$$w^p_1 = -(r/(2\pi)^{1/2}\omega)J_{n+1}(\omega r)/J_{n+1}(\omega)[(\mu c_c + \eta a_c)\cos n\theta + (\mu c_s + \eta a_s)\sin n\theta], \tag{68}$$

$$w^p_2 = -\frac{\mu r}{2\omega} \sum_{j=0, j \neq n}^{\infty} J_{j+1}(\omega r)[B_j \cos j\theta + C_j \sin j\theta], \tag{69}$$

$$w^p_3 = -\frac{\mu^2 r}{(32\pi)^{1/2}\omega^3 J_{n+1}(\omega)}[\omega r J_n(\omega r) - 2(n+1)J_{n+1}(\omega r)](a_c \cos n\theta + a_s \sin n\theta), \tag{70}$$

$$w^p = w^p_1 + w^p_2 + w^p_3, \qquad w^h = \sum_{j=0, j \neq n}^{\infty} J_j(\omega r)[E_j \cos j\theta + F_j \sin j\theta]. \tag{71, 72}$$

Components w_i^p are associated with the three inhomogeneities of equation (16a) resulting from an expansion analogous to equation (47). The particular solution (71) is the essential element allowing calculation of the E_j and F_j from equation (16b).

4.2.3. Third order perturbation

The solvability conditions for equations (17) and (11b) give

$$
\begin{bmatrix} \mu + \omega^2 g_{2n}^c & \omega^2 g_{2n}^s & \omega^2 a_c \\ \omega^2 g_{2n}^s & \mu - \omega^2 g_{2n}^c & \omega^2 a_s \\ \omega^2 a_c & \omega^2 a_s & 0 \end{bmatrix} \begin{Bmatrix} d_c \\ d_s \\ \kappa/\omega^2 \end{Bmatrix} = \begin{Bmatrix} -\mu\langle u^c, w^p \rangle - \eta\langle u^c, v \rangle - \tilde{J}(u^c, s) \\ -\mu\langle u^s, w^p \rangle - \eta\langle u^s, v \rangle - \tilde{J}(u^s, s) \\ -\omega^2[\tfrac{1}{2}\langle v, v \rangle + a_c\langle u^c, w^p \rangle + a_s\langle u^s, w^p \rangle] \end{Bmatrix}.
$$

(73)

The operator in equation (73) is identical to that in equation (63), and the assumption of first order eigenvalue splitting ensures its invertibility in the calculation of d_c, d_s, and κ.

The third order eigenfunction perturbation $s(r, \theta)$ is

$$
s = e_c u^c + e_s u^s + s^h + s^p,
$$

(74)

$$
s_1^p = -\frac{r}{(2\pi)^{1/2}\omega} \frac{J_{n+1}(\omega r)}{J_{n+1}(\omega)} [(\mu d_c + \eta c_c + \kappa a_c) \cos n\theta + (\mu d_s + \eta c_s + \kappa a_s) \sin n\theta],
$$

(75)

$$
s_2^p = -\frac{\eta r}{2\omega} \sum_{j=0, j \neq n}^{\infty} J_{j+1}(\omega r) [B_j \cos j\theta + C_j \sin j\theta],
$$

(76)

$$
s_3^p = -\frac{\mu n r}{(32\pi)^{1/2}\omega^3 J_{n+1}(\omega)} [\omega r J_n(\omega r) - 2(n+1)J_{n+1}(\omega r)] (a_c \cos n\theta + a_s \sin n\theta),
$$

(77)

$$
s_4^p = -\frac{\mu r}{2\omega} \sum_{j=0, j \neq n}^{\infty} J_{j+1}(\omega r) [E_j \cos j\theta + F_j \sin j\theta],
$$

(78)

$$
s_5^p = -\frac{\mu r}{(32\pi)^{1/2}\omega^3 J_{n+1}(\omega)} [\omega r J_n(\omega r) - 2(n+1)J_{n+1}(\omega r)]
$$

$$
\times ((\mu c_c + \eta a_c) \cos n\theta + (\mu c_s + \eta a_s) \sin n\theta),
$$

(79)

$$
s_6^p = -\frac{\mu^2 r}{8\omega^3} \sum_{j=0, j \neq n}^{\infty} [\omega r J_j(\omega r) - 2(j+1)J_{j+1}(\omega r)] (B_j \cos j\theta + C_j \sin j\theta),
$$

(80)

$$
s_7^p = \frac{\mu^3 r(n+2)}{(288\pi)^{1/2}\omega^4 J_{n+1}(\omega)} \left[r J_n(\omega r) + \frac{r^2\omega^2 - 4(n+1)}{2\omega} J_{n+1}(\omega r) \right] (a_c \cos n\theta + a_s \sin n\theta),
$$

(81)

$$
s^p = s_1^p + s_2^p + s_3^p + s_4^p + s_5^p + s_6^p + s_7^p,
$$

(82)

$$
s^h = \sum_{j=0, j \neq n}^{\infty} J_j(\omega r) [H_j \cos j\theta + L_j \sin j\theta],
$$

(83)

where the H_j, L_j follow from equation (17b).

4.2.4. *Fourth order perturbation*

From the solvability conditions for equations (18) and (11c),

$$
\begin{bmatrix}
\mu + \omega^2 g_{2n}^c & \omega^2 g_{2n}^s & \omega^2 a_c \\
\omega^2 g_{2n}^s & \mu - \omega^2 g_{2n}^c & \omega^2 a_s \\
\omega^2 a_c & \omega^2 a_s & 0
\end{bmatrix}
\begin{Bmatrix}
e_c \\
e_s \\
\chi/\omega^2
\end{Bmatrix}
$$

$$
= \begin{Bmatrix}
-\mu\langle u^c, s^p\rangle - \eta\langle u^c, w\rangle - \kappa\langle u^c, v\rangle - \tilde{J}(u^c, t) \\
-\mu\langle u^s, s^p\rangle - \eta\langle u^s, w\rangle - \kappa\langle u^s, v\rangle - \tilde{J}(u^s, t) \\
-\omega^2[\langle v, w\rangle + a_c\langle u^c, s^p\rangle + a_s\langle u^s, s^p\rangle]
\end{Bmatrix}. \quad (84)
$$

5. EXAMPLE PROBLEMS

The numerical accuracy achievable by the presented method is illustrated by modeling elliptical and rectangular domains with a circle.

5.1. ELLIPTICAL DOMAIN

An elliptical domain of eccentricity $e = (1 - b^2/a^2)^{1/2}$ is described by

$$
R = a[(1 - e^2)/(1 - e^2 \cos^2 \theta)]^{1/2}, \quad (85)
$$

where a and b are the semi-major and semi-minor axes, respectively (Figure 2). The average radius $\bar{R}$ (equation (3b)) and the Fourier coefficients of $g(\theta)$ (equation (24)) are calculated by quadrature. Though $\bar{R}$ depends on a and e, $g(\theta)$ depends only on e. For an ellipse, $g_j^c = 0$ for j odd and $g_j^s = 0$ for all j. Eight non-trivial terms through g_{16}^c were used in the calculations.

The dimensionless, fundamental, elliptical domain eigenvalue $\Omega_{00} a$ of equation (2) evolves from the fundamental circular domain eigenvalue. (One identifies the perturbed domain eigensolutions using subscripts mn denoting the number of nodal circles m and nodal diameters n in the circular domain eigensolutions from which the perturbed eigensolutions evolve.) Table 1 compares the fundamental eigenvalue predicted by perturbation to the exact values computed by Daymond [13]. A maximum error of 0.32% is calculated for eccentricities through $e = 0.9 \rightarrow b/a = 0.4539$. For the extreme eccentricity $e = 0.9611 \rightarrow b/a = 0.28$, the perturbation results degrade substantially. Even without comparison with a known solution, the degradation is evident by the poor convergence
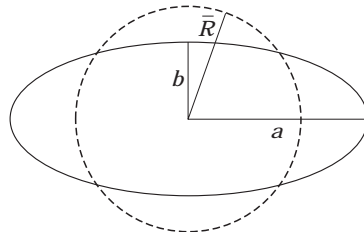

Figure 2. Ellipse of eccentricity $e = 0.9$ ($b/a = 0.4359$). The circle is the base domain for the perturbation. The radius of the circle equals the average radius of the ellipse.

TABLE 1

Comparison of the fundamental elliptical domain eigenvalue $\Omega_{00}a$ computed using perturbation to the exact solution of Daymond [13]. Perturbed eigenvalues $(\Omega_{01}a)_{1,2}$ evolving from the 0 nodal circle, 1 nodal diameter circular domain eigenvalues are also presented. $e = (1 - b^2/a^2)^{1/2}$ denotes the eccentricity of the ellipse. Numbers in parentheses indicate the order of perturbation.

		e						
		0·4	0·5	0·6	0·7	0·8	0·9	0·9611
$\Omega_{00}a$	Exact	2·5165	2·5968	2·7202	2·9215	3·2933	4·2151	6·2432
	pert. (5)	2·5165	2·5968	2·7202	2·9215	3·2936	4·2287	7·2790
	% Error	0·00	0·00	0·00	0·00	0·01	0·32	17
$(\Omega_{01}a)_1$	Pert. (4)	3·9212	3·9864	4·0878	4·2559	4·5726	5·3318	—
$(\Omega_{01}a)_2$	Pert. (4)	4·0956	4·2822	4·5646	5·0154	5·8259	7·7601	—

of the perturbation with increasing order. For $e = 0.9611$, the asymptotic expansion (9) for the fundamental frequency is

$$\bar{\omega}^2 = 5\cdot7831 + 0 + 5\cdot1154 - 5\cdot3966 + 4\cdot7782 + 1\cdot7258,$$

$$(\Omega_{00}\, a) = \bar{\omega}/\bar{R}_{a=1} = 3\cdot4650/0\cdot47603 = 7\cdot2790.$$

In contrast, for $e = 0.9$,

$$\bar{\omega}^2 = 5\cdot7831 + 0 + 1\cdot6774 - 0\cdot6083 + 0\cdot3098 - 0\cdot0005,$$

$$(\Omega_{00}\, a) = \bar{\omega}/\bar{R}_{a=1} = 2\cdot6761/0\cdot63284 = 4\cdot2287.$$

The agreement between perturbation and the exact values is illustrated in Figure 3. Results for perturbation of the one nodal diameter circular domain eigenvalue are also given in Figure 3, where the exact values were obtained by optically scanning Figure 1 of Troesch
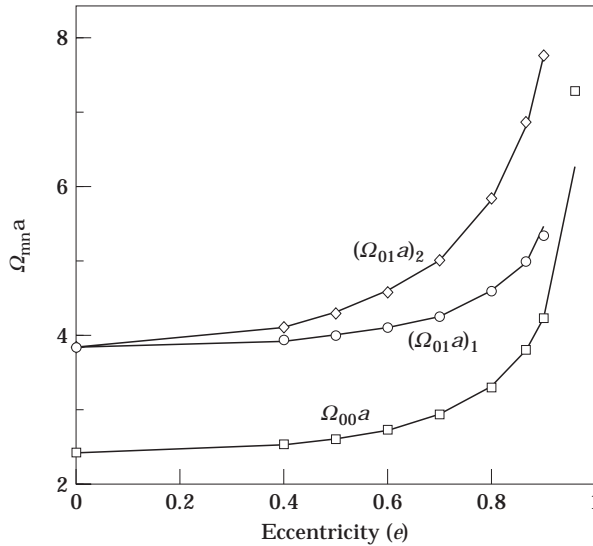

Figure 3. Elliptical domain eigenvalues. The subscript *mn* denotes the number of nodal circles (*m*) and nodal diameters (*n*) in the circular domain ($e = 0$) eigenvalue. *a* is the semi-major axis length of the ellipse. The solid lines are determined from the exact solutions of Daymond [13] and Troesch and Troesch [14]. The symbols are values predicted by perturbation.
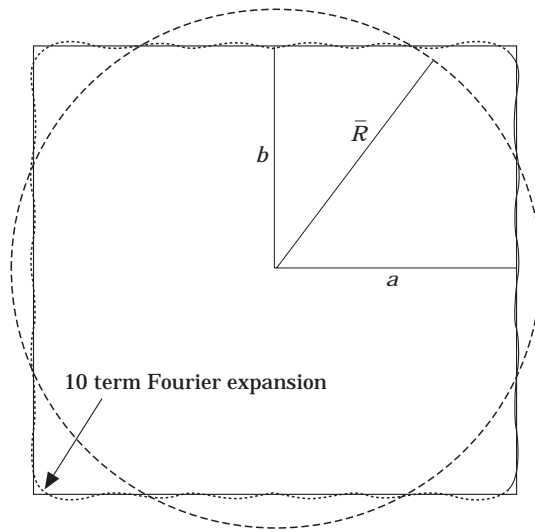
Figure 4. Rectangle of aspect ratio $\xi = 0\cdot9$. The approximate rectangle (dotted line) is a 10 term Fourier approximation of the rectangle. The circle is the base domain of the perturbation. The radius of the circle equals the average radius of the rectangle.

and Troesch [14] and digitizing points through $e = 0\cdot9$. Differences between the results so obtained and the perturbation values are all less than 3%, which is approximately the precision of the scanned and digitized results. Tabular results for the $(\Omega_{01} a)_{1,2}$ eigenvalues are presented in Table 1.

5.2. RECTANGULAR DOMAIN

Consider the rectangular domain of dimension $2a \times 2b$ where $\xi = b/a \leqslant 1$ (Figure 4). The average radius $\bar{R}$ and the Fourier coefficients of $g(\theta)$ are calculated by quadrature.
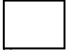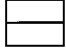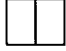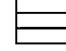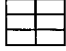
TABLE 2

Comparison of the fundamental rectangular domain eigenvalue computed using perturbation to exact values. $\xi = b/a$ denotes the aspect ratio of the rectangle. The numbers in parentheses indicate the order of perturbation.

	ξ							
$\Omega_{00}a$	1	0·9	0·8	0·7	0·6	0·5	0·4	0·3
Exact	2·2214	2·3481	2·5145	2·7391	3·0531	3·5124	4·2295	5·4665
Pert. (5)	2·2243	2·3511	2·5183	2·7460	3·0665	3·5597	4·4293	6·6599
% Error	0·13	0·13	0·15	0·25	0·44	1·3	4·7	22
Pert. (4)	2·2193	2·3455	2·5109	2·7325	3·0409	3·4797	4·1413	4·9888
% Error	−0·10	−0·11	−0·14	−0·24	−0·40	−0·93	−2·1	−8·7
Pert. (3)	2·2127	2·3394	2·5027	2·7230	3·0278	3·4672	4·0995	4·9403
% Error	−0·40	−0·37	−0·47	−0·59	−0·83	−1·3	−3·1	−9·6
Pert· (2)	2·2479	2·3753	2·5430	2·7700	3·0923	3·5830	4·4038	5·9903
% Error	1·2	1·2	1·1	1·1	1·3	2·0	4·1	9·6
Pert. (1)	2·1430	2·2608	2·4049	2·5859	2·8209	3·1400	3·6013	4·3353
% Error	−3·5	−3·7	−4·4	−5·6	−7·6	−11	−15	−21

TABLE 3

Comparison of the rectangular domain eigenvalues $\Omega_{mn}a$ computed using perturbation to exact values. $\xi = b/a \leqslant 1$ is the rectangle aspect ratio. m and n are the numbers of nodal circles and nodal diameters, respectively, in the circular domain eigenfunction from which the corresponding rectangular domain eigenfunction evolves.

ξ		m, n							
		$(0, 0)$	$(0, 1)_1$	$(0, 1)_2$	$(0, 2)_2$	$(0, 2)_1$	$(1, 0)$	$(0, 3)_1$	$(0, 3)_2$
1	Exact	2·2214	3·5124	3·5124	4·4429	4·9673	4·9673	5·6636	5·6636
	Pert.	2·2243	3·5081	3·5123	4·4322	4·9679	4·9656	5·7064	5·7071
	% Err.	0·13	−0·12	0·00	−0·24	0·01	−0·03	0·76	0·76
0·95	Exact	2·2806	3·5502	3·6610	4·5613	4·9941	5·2032	5·7569	5·8716
	Pert.	2·2836	3·5442	3·6553	4·5499	5·0136	5·2027	5·8693	5·8873
	% Err.	0·13	−0·17	−0·16	−0·25	0·39	0·00	2·0	0·27
0·9	Exact	2·3481	3·5939	3·8278	4·6962	5·0252	5·4665	5·8644	6·1062
	Pert.	2·3511	3·5879	3·8218	4·6831	4·9148	5·5454	6·1071	6·1390
	% Err.	0·13	−0·17	−0·16	−0·28	−2·2	1·4	4·1	0·54
0·8	Exact	2·5145	3·7047	4·2295	5·0290	5·1051	6·0963	6·1342	6·6759
	Pert.	2·5183	3·6984	4·2219	5·0063	5·0071	3·9446	6·6318	6·7169
	% Err.	0·15	−0·17	−0·17	−0·45	−1·9	−35	8·1	0·61
0·7	Exact	2·7391	3·8607	4·7549	5·4783	5·2194	6·9128	6·5076	7·4289
	Pert.	2·7460	3·8493	4·7478	5·4315	8·7571	imag	6·1737	7·0269
	% Err.	0·25	−0·29	−0·15	−0·85	68	—	−5·1	−5·4

$\bar{R}$ depends on a and ξ, but $g(\theta)$ depends only on ξ. Also, $g_j^c = 0$ for j odd and $g_j^s = 0$ for all j. Ten non-trivial terms through g_{20}^c were used in the calculations (Figure 4).

Table 2 compares the fundamental eigenvalue $\Omega_{00}\,a$ from perturbation to the exact value for $1 \geqslant \xi \geqslant 0\cdot3$. Comparisons are shown for first–fifth order perturbation approximations. For a fifth order perturbation approximation, errors in the fundamental frequency are less than 0·5% for $\xi \geqslant 0\cdot6$, 1·3% for $\xi = 0\cdot5$, and 4·7% for $\xi = 0\cdot4$. For $\xi = 0\cdot3$, the error is 22·0% and perturbation is not effective. The behavior of the asymptotic approximation (vertical column of Table 2) reveals a large expected error even in the absence of a known solution.

Substantial improvement in the predicted fundamental eigenvalue results when the perturbation is extended from first to second order. The accuracy obtainable from a second order perturbation is significant because the closed form expression (33) gives η for an arbitrary shape perturbation. Improved accuracies are achieved with third order and fourth order perturbations. For rectangular domains, fifth order perturbation affords no increase in accuracy. Though the accuracy achieved using fourth or fifth order perturbation may not be needed, the higher order perturbations develop confidence in the convergence of the predicted eigensolutions through the decreased magnitude of the higher order terms.

Comparisons of perturbation predictions and exact eigenvalues are shown in Table 3 for rectangular domains. For square domains, all predicted values differ from the exact values by less than 1%, and the agreement is also excellent for $\xi = 0\cdot95$ and $\xi = 0\cdot9$. The lowest four eigenvalues provide excellent estimates for $\xi = 0\cdot7, 0\cdot8$, as shown in Figure 5. Where the predicted and exact values differed substantially, the failure of the higher order perturbations to approach zero in the asymptotic expansion is evident.
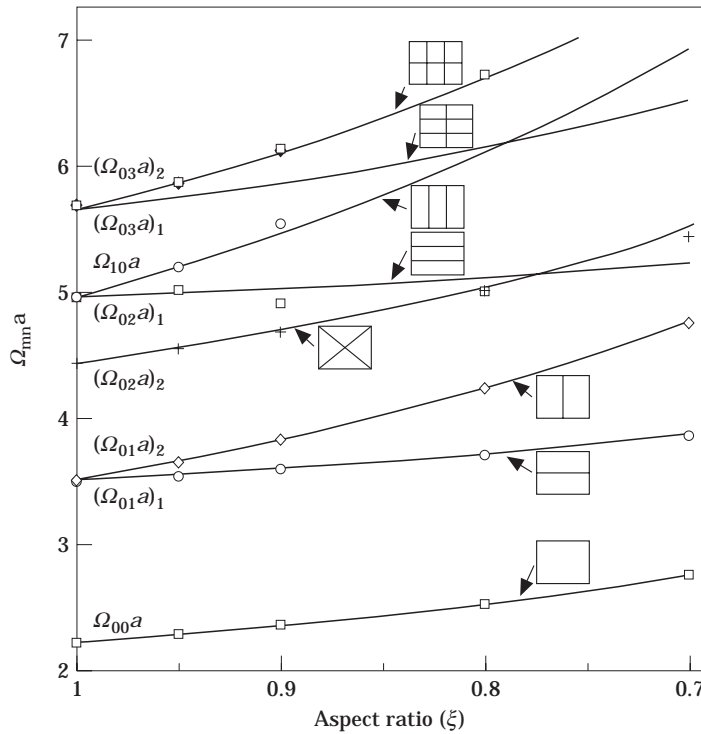
Figure 5. Eigenvalues of a rectangular domain with aspect ratio $\xi = b/a$. Solid curves denote exact values. Symbols denote values predicted by perturbation.

It is interesting that two distinct circular domain eigenvalues can merge to form a degenerate eigenvalue pair on a square domain. For instance, the $(m, n) = (1, 0)$ circular domain eigenvalue and one of the degenerate $(m, n) = (0, 2)$ circular domain eigenvalues merge to form the degenerate eigenvalue pair $\Omega a = 4 \cdot 9673$ in the square domain. In contrast, the degenerate eigenvalue pairs $\Omega a = 3 \cdot 5124$ and $\Omega a = 5 \cdot 6636$ in the square domain evolve from the degenerate eigenvalue pairs $(m, n) = (0, 1)$ and $(m, n) = (0, 3)$ in the circular domain. Perturbation predicts the splitting of the degenerate square domain eigenvalues (Figure 5).

6. DISCUSSION

The presented boundary perturbation method applies for general boundary conditions of the form of equations (7b, c). For annular domains, the Bessel function $Y_n (\omega_{mn} r)$ is included in equations (20, 21); particular solutions associated with this additional term are almost identical to those associated with $J_n (\omega_{mn} r)$ [10]. If different unperturbed boundary conditions are considered, the unperturbed eigenfunctions (20, 21) do not change form; only the normalization coefficients change. Consequently, the form of the right side of equation (15a) is unchanged, and the particular solutions (29, 60) apply except for a change in their leading coefficients. Different first order boundary condition perturbations $\bar{C}$ and $\hat{C}$ change only the values of the coefficients B_j and C_j in equations (30, 61). Instead of equation (15b), these coefficients are determined by the general perturbed boundary condition (7c),

$$[v^h + \beta_o v_r^h]_{\partial P} = -\hat{C}u - [v^p + \beta_o v_r^p]_{\partial P}. \tag{86}$$

Calculation of B_j and C_j is always possible by Fourier expansion of equation (86). Thus, the forms of v in equations (28) and (59) are unaffected by changes in either the perturbed or unperturbed boundary operators. As a result, only coefficients of the particular solutions (35, 71) change for different boundary conditions. This reasoning extends to higher order perturbations, and consequently the presented particular solutions admit exact eigensolution perturbations for general boundary condition perturbations.

Boundary condition perturbation offers an attractive combination of analytical and computational advantages. The closed form expressions show explicit dependence of the eigenvalues on parameters. The simplicity of these expressions for arbitrary circumferential distribution of the perturbation allows ready assessment of qualitative and quantitative eigensolution changes induced by a given asymmetry distribution. The simplicity also permits convenient use of the eigensolutions in applications such as inverse problems, forced and transient response calculations, and system identification. Kac posed an inverse problem: 'Can one hear the shape of a drum?' [15]. Use of the general formulae for the eigensolutions in terms of the Fourier coefficients of the boundary asymmetry and an optimization procedure could address this problem. Derivation, use, and verification of the results can be automated using computer algbera software, thereby minimizing programming errors. Boundary condition perturbation can handle more general asymmetries than Ritz–Galerkin analyses because no admissible functions are required. The magnitude of asymmetry for which accurate solutions are obtainable is remarkably large for a perturbation solution. Substantial errors are possible, however, as seen in the higher eigenvalues for rectangular domains. Accuracy limitations increase as higher eigenvalues are considered.

7. CONCLUSIONS

(1) Eigensolutions of the wave equation with perturbations of the boundary conditions are derived by exact solution of the sequence of perturbation problems up to fifth order. Perturbations of the domain from circular and variation of boundary condition parameters along the boundary curves are included in the class of perturbations for which the method applies. Exactness of the perturbation solutions means no approximation is introduced other than truncation of the asymptotic series equations (9, 10).

(2) The derived solution offers a combination of analytical and computational advantages: exact perturbation through fifth order yields excellent accuracy for perturbations of substantial magnitude (such as the elliptical and rectangular domain perturbation examples); Fourier representation of the perturbations allows treatment of general continuous or discontinuous asymmetries; algebraic simplicity of the results permits convenient use of the eigensolutions in applications such as inverse and forced response problems; results are easily derived and verified using computer algebra software.

(3) Rules governing splitting of the degenerate unperturbed eigenvalues are derived at both first and second orders of perturbation. These rules take simple algebraic forms in terms of the Fourier coefficients of a general asymmetry. The rule for first order eigenvalue splitting is such that it can be applied by inspection.

REFERENCES

1. J. R. KUTTLER and V. G. SIGILLITO 1984 *SIAM Review* **26**, 163–193. Eigenvalues of the Laplacian in two dimensions.
2. J. MAZUMDAR 1975 *Shock and Vibration Digest* **7**, 75–88. A review of approximate methods for determining the vibrational modes of membranes.

3. J. Mazumdar 1979 *Shock and Vibration Digest* **11**, 25–29. A review of approximate methods for determining the vibrational modes of membranes.
4. J. Mazumdar 1982 *Shock and Vibration Digest* **14**, 11–17. A review of approximate methods for determining the vibrational modes of membranes.
5. S. B. Roberts 1967 *Journal of Applied Mechanics* **34**, 618–622. The eigenvalue problem for two-dimensional regions with irregular boundaries.
6. D. D. Joseph 1967 *Archives of Rational Mechanics and Analysis* **24**, 325–351. Parameter and domain dependence of eigenvalues of elliptic partial differential equations.
7. J. Mazumdar 1973 *Journal of Sound and Vibration* **27**, 47–57. Transverse vibration of membranes of arbitrary shape by the method of constant deflection contours.
8. P. M. Morse and H. Feshbach 1953 *Methods of Theoretical Physics*. New York: McGraw-Hill.
9. A. H. Nayfeh 1981 *Introduction to Perturbation Techniques*. New York: J. Wiley.
10. R. G. Parker and C. D. Mote, Jr. 1996 *Journal of Applied Mechanics* **63**, 128–135. Exact boundary condition perturbation solutions in eigenvalue problems.
11. R. G. Parker and C. D. Mote, Jr 1996 *Journal of Applied Mechanics*. Exact higher order boundary condition perturbation in eigenvalue problems.
12. R. G. Parker and C. D. Mote, Jr. 1996 *Journal of Vibration and Acoustics* **118**, 436–445. Exact perturbation for the vibration of almost annular or circular plates.
13. S. D. Daymond 1955 *Quarterly Journal of Mechanics and Applied Mathematics* **VIII**, 361–372. The principal frequencies of vibrating systems with elliptic boundaries.
14. B. A. Troesch and H. R. Troesch 1973 *Mathematics of Computation* **27**, 755–765. Eigenfrequencies of an elliptic membrane.
15. M. Kac 1966 *American Mathematics Monthly* **73**, 1–23. Can one hear the shape of a drum?